Photofragment angular momentum distributions in the molecular frame. II. Single state dissociation, multiple state interference, and nonaxial recoil in photodissociation of polyatomic molecules

Photofragment angular momentum distributions in the molecular frame. II. Single state dissociation, multiple state interference, and nonaxial recoil in photodissociation of polyatomic molecules

T. Peter Rakitzis and Andrew J. Alexander

Citation: J. Chem. Phys. **132**, 224310 (2010); doi: 10.1063/1.3429744
View online: http://dx.doi.org/10.1063/1.3429744
View Table of Contents: http://jcp.aip.org/resource/1/JCPSA6/v132/i22
Published by the AIP Publishing LLC.

Photofragment angular momentum distributions in the molecular frame. II. Single state dissociation, multiple state interference, and nonaxial recoil in photodissociation of polyatomic molecules

T. Peter Rakitzis[1,a)] and Andrew J. Alexander[2]
[1]*Department of Physics, University of Crete, Heraklion 71110, Crete, Greece and Institute of Electronic Structure and Laser, Foundation for Research and Technology-Hellas, Heraklion 71110, Crete, Greece*
[2]*School of Chemistry, University of Edinburgh, West Mains Road, Edinburgh EH9 3JJ, United Kingdom*

(Received 2 January 2010; accepted 23 April 2010; published online 11 June 2010)

We present an $a_q^k(s)$ polarization-parameter model to describe product angular momentum polarization from the one-photon photodissociation of polyatomic molecules in the molecular frame. We make the approximation that the final photofragment recoil direction is unique and described by the molecular frame polar coordinates (α,φ_i), for which the axial recoil approximation is a special case (e.g., $\alpha=0$). This approximation allows the separation of geometrical and dynamical factors, in particular, the expression of the experimental sensitivities to each of the $a_q^k(s)$ in terms of the molecular frame polar angles (χ_i,φ_i) of the transition dipole moment $\boldsymbol{\mu}_i$. This separation is applied to the linearly polarized photodissociation of polyatomic molecules (asymmetric, symmetric, and spherical top molecules are discussed) and to all dissociation mechanisms that satisfy our recoil approximation, including those with nonaxial recoil and multiple state interference, giving important insight into the geometrical properties of the photodissociation mechanism. For example, we demonstrate that the ratio of polarization parameters $A_0^k(\text{aniso})/A_0^k(\text{iso})=\beta$ (where β is the spatial anisotropy parameter) is an indication that the dynamics can be explained by a single dissociative state. We also show that for asymmetric top photodissociation, the sensitivity to the $a_1^k(s)$ parameters, which can arise either from single-surface or multiple-surface interference mechanisms, is nonzero only for components of the transition dipole moments within the **v**-**d** plane of the recoil frame. © *2010 American Institute of Physics*. [doi:10.1063/1.3429744]

I. INTRODUCTION

For several decades, information about the photodissociation process in the molecule frame has been obtained from the measurement of laboratory-frame vector properties.[1–4] The most well-known example has been the measurement of the angular distribution of photofragments from isotropic parent molecules, with respect to the photolysis laser polarization,[5]

$$I(\varepsilon) = 1 + \beta P_2(\cos\varepsilon), \tag{1}$$

where ε is the angle between the recoil direction **v** and the direction **E** of the polarization of the photodissociating light, and P_2 is the second-order Legendre polynomial (note that this equation is valid only for one-photon photodissociation in the dipole approximation). In the case where photodissociation occurs promptly via a single dissociative state, then the parameter β, in Eq. (1), is given by the particularly simple expression[5–7]

$$\beta = 2P_2(\cos\chi), \tag{2}$$

where χ is the angle between the recoil direction **v** and the transition dipole moment $\boldsymbol{\mu}$ of the dissociating state. It is worth noting that this expression is correct even if the dissociation is not axial so that the original bond direction and the final recoil direction are not parallel; therefore, the angle between the original bond direction and $\boldsymbol{\mu}$ can only be inferred. The one-to-one correspondence between β and χ shown by Eq. (2) no longer holds if there are more than one dissociative state of different symmetries, or if the lifetime of a predissociative state is comparable or longer than the rotational period of the parent molecule. Therefore, Eq. (2) can be used to determine χ directly (without other information) only for cases when it is known that photodissociation occurs via only one dissociative state. The case of at least two dissociative states, for which there are at least two angles χ_1 and χ_2 (for prompt dissociation, and in the high-J limit), can be unraveled by studying the angular distribution of oriented parent molecules.[8,9]

Photofragment angular momentum distributions possess significant dynamical information which can be measured to elucidate the details of the photodissociation dynamics.[10] In 1994, Siebbeles *et al.*[11] presented a quantum treatment of the laboratory-frame angular momentum distribution of photofragments in the axial recoil limit, which treated the coherent excitation of dissociative states of well-defined helicity. This treatment was very well suited for the description of the angular momentum distribution of photofragments from the prompt photodissociation of diatomic molecules. A few years later, Rakitzis and Zare[12] developed a phenomenological molecular frame description of the photofragment angular mo-

a)Electronic mail: ptr@iesl.forth.gr.

mentum distributions equivalent to the description of Siebbeles *et al.*, which also gave explicit expressions for experimental detection of the polarization parameters $a_q^k(p)$ [the label (p) refers to the symmetry of the transitions excited: parallel $(\parallel)$, perpendicular $(\perp)$, or mixed $(\parallel,\perp)$].[12–14] Molecule-frame photofragment polarization formalisms have now been applied to several cases with considerable success, in particular, to the study of the prompt photodissociation of the diatomic molecules Cl_2,[15–20] ICl,[21–23] HCl,[24,25] HBr,[26] BrCl,[27,28] O_2,[29,30] and RbI.[31–33] It was shown that the photofragment angular momentum distributions could indeed be decomposed into incoherent contributions for parallel and perpendicular transitions [described by the parameters $a_0^k(\parallel)$, and $a_0^k(\perp)$ and $a_2^k(\perp)$, respectively], and also the coherent contributions from interference between the parallel and the perpendicular transitions [described by the $a_1^k(\parallel,\perp)$ parameters]. Some key outcomes of these studies included the following.

(a) The observation of Cl-photofragment orientation from the photodissociation of ICl with linearly polarized light, described by the $\mathrm{Im}[a_1^1(\parallel,\perp)]$ parameter.[22,23] The value of this parameter was observed to oscillate sinusoidally as a function of the photolysis wavelength, affording a direct measurement of the phase shift between the asympototic wavefunctions associated with dissociative parallel and perpendicular transitions. The analysis of this wavelength-dependent polarization oscillation allowed the determination of the shapes of the potential energy surfaces of the two relevant dissociative states to better than 30 cm^{-1} Å.[34] Similarly, Korovin *et al.*[33] measured the phase shift between a parallel and perpendicular transition for RbI using circularly polarized light.

(b) The observation of nonadiabatic transfer at long range, in the cases of Cl_2,[15–17,20,35] ICl,[21,34] BrCl,[18,27,28] and O_2,[29,30] as inferred from the values of incoherent parameters, $a_0^k(\parallel)$, $a_0^k(\perp)$, and $a_2^k(\perp)$. Evidence for such nonadiabatic transfer can only be observed from the photofragment angular momentum distributions.

(c) The measurement of all the alignment parameters for the Cl and Br photofragments from the photodissociation, at 193 nm, of HCl and HBr,[24–26,36,37] respectively, and the excellent agreement with scattering calculations from potential energy surfaces calculated *ab initio*.[38,39]

(d) The production of highly polarized atoms at high density from molecular photodissociation, which can be used for the study of polarization effects in collision experiments. Nearly maximally polarized $O(^1D)$ atoms were produced from the photodissociation of O_2 (with nearly 100% of the population in the $m=0$ state),[40] and highly spin-polarized H atoms were produced from the photodissociation of HCl and HBr.[24–26,36,37] In addition, atoms with significant polarization were produced in most cases where molecules were photodissociated to produce atomic photofragments (see Refs. 15–40).

The considerable success of the treatment of photofragment angular momentum distribution in the case of diatomic molecules, in particular, the excellent agreement between theory and experiment, gives the justified impression that the photodissociation of diatomic molecules is largely understood, even at this extremely detailed level.[10] The Siebbeles and $a_q^k(p)$ polarization molecule-frame parameter formalisms span the complete space of experimental signals for the one-photon photodissociation of any molecule yielding two fragments so that all possible experimental polarization signals can be fit with the complete set of $a_q^k(p)$ polarization parameters. However, the interpretations of the $a_q^k(p)$ polarization parameters, which are so appealing in the case of diatomic-molecule photodissociation, are not as well defined in the case of the photodissociation of polyatomic molecules.

Photofragment alignment has been studied for a number of triatomic and polyatomic molecules, in particular, the correlation between the product velocity and angular momentum vectors (**v**-**J** correlation).[2,3,41,42] Recent work focused on measurement of molecule-frame polarization parameters in the photodissociation of several polyatomic molecules, such as ICN,[43–48] NO_2,[49–53] OCS,[54–60] N_2O,[61–65] O_3,[66–73] H_2O_2,[74,75] and SO_2.[76] For example, the polarization of the $S(^1D)$ atoms from the photodissociation of OCS has been measured by a number of groups, and large values for the $a_1^k(\parallel,\perp)$ parameters (such as the $\mathrm{Im}[a_1^1(\parallel,\perp)]$, $\mathrm{Re}[a_1^2(\parallel,\perp)]$, and $\mathrm{Re}[a_1^4(\parallel,\perp)]$) have been observed.[56–59] In the case of diatomic photodissociation, the values of these parameters would be interpreted to indicate the presence of interference between at least one parallel and one perpendicular transition (and the phase shift between two such interfering states could be determined). These $q=1$ parameters arise from a transition dipole moment that is at an intermediate angle to the final recoil direction (different from 0° or 90°). In the case of the prompt photodissociation of a diatomic molecule, such an angle χ can be obtained only by the coherent excitation of a pure parallel and perpendicular transition; that is why, for the photodissociation of diatomic molecules, the observation of the $q=1$ parameters constitutes a definitive signature of the interference of dissociative states of different symmetries. In contrast, the excited state of a polyatomic molecule that does not possess cylindrical symmetry can, in general, possess a transition dipole moment that is at an angle χ to the final photofragment recoil direction.

The aim of this paper is to introduce a model, based on an $a_q^k(s)$ polarization-parameter formalism [extending the $a_q^k(p)$ formalism] to fit generally the angular momentum distributions of photofragments from the prompt photodissociation of isotropic polyatomic molecules via excitation to one or two electronics states, within the limits of the unique-recoil destination (URD) approximation. Predissociation is not dealt with here, but the $a_q^k(s)$ formalism could be extended to treat predissociation as well; Vasyutinskii and co-workers[77–81] examined the effect of parent molecule rotation and predissociation on the photofragment polarization, and showed that the polarization parameters are reduced. The label (s) refers to the excited electronic states that produced the photofragment polarization being described by the $a_q^k(s)$ parameter; for example, for photodissociation via states A and B, $a_q^k(A)$ and $a_q^k(B)$ describe photofragment polarization from dissociation via states A and B, respectively, whereas

$a_q^k(A,B)$ describes photofragment polarization that arises from the coherent excitation of states A and B.

The main approximation we make is the URD approximation, which is an extension of the axial recoil approximation, and allows separation between the purely geometrical aspects of the photodissociation [described by the angles between the final recoil direction **v** and transition dipole moments $\boldsymbol{\mu}_i$, given by the molecular frame coordinates (χ_i,φ_i)] and the dynamical aspects [described by the $a_q^k(s)$]. In particular, we show how the sensitivity to each of the $a_q^k(s)$ parameters depends on the (χ_i,φ_i), while also giving some physical interpretation to the $a_q^k(s)$ based on their symmetry properties. We consider dissociation via a single dissociative state and also consider the interference from multiple dissociative states. Comparing these two cases, we discuss when a single dissociative surface suffices to explain experimental signals, or when multiple dissociative surfaces are necessary. Our model of the photofragment angular momentum distributions is functionally equivalent to the (complete basis) bipolar moment expansion of Dixon; Vasyutinskii and co-workers[77,79] also presented general laboratory-frame expansions.

The equations describing the photofragment angular momentum distributions in the molecule frame for single and multiple dissociative states are presented and discussed in Secs. II A and II B, respectively, whereas general expressions are given in Sec. II C. In Sec. II D, transformation equations are given which allow the description of the full three-dimensional angular momentum distributions in the laboratory frame. In Sec. II E we derive and tabulate useful expressions for the detection sensitivity factors s_k of the polarization parameters for $2+1$ resonance enhanced multiphoton ionization (REMPI), and the physical limits of the polarization parameters as a function of the quantum number J. In Appendixes A and B, we present the physical limits of the a_0^k polarization parameters for the case of $J=3$, and we show how the laboratory angular momentum distribution can be calculated from the molecular frame equations, for particular widely used experimental measurement schemes such as slice imaging with the Doppler detection.

II. THEORY

A. Single surface dissociation

We consider the photodissociation of a polyatomic molecule M-N, with a principal symmetry axis **d** (the case of spherical top molecules is discussed later), which yields photofragments M and N, which can each be either atomic or polyatomic photofragments. We will consider the angular momentum of the M photofragments, which have angular momentum **J**. The probability of absorbing the photodissociating photon is proportional to $|\boldsymbol{\mu}_i\cdot\mathbf{E}|^2$, where $\boldsymbol{\mu}_i$ is the transition dipole moment for excitation from the initial electronic state to the dissociative state i, and **E** is the polarization direction of the linearly polarized photolysis light. After photodissociation, the photofragment M has recoil velocity **v**, which we take to be parallel to the recoil-frame z-axis

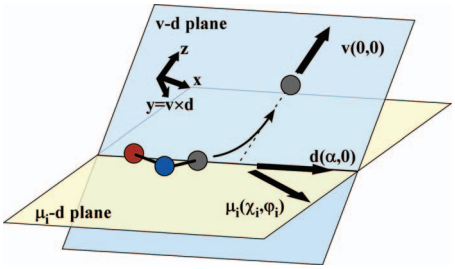

FIG. 1. Polar coordinates of the dynamical vectors (**v**, $\boldsymbol{\mu}_i$, and **d**) for the photodissociation of an asymmetric top molecule, showing that the recoil frame (defined by **v** and **d**) is not necessarily parallel to the initial molecular frame (defined by $\boldsymbol{\mu}_i$ and **d**).

(irrespective of whether the recoil was axial or not). The y-axis is defined by $\mathbf{v}\times\mathbf{d}$ and the x-axis is in the **v**-**d** plane (see Fig. 1).

We make the following main approximation, which we call the URD approximation: In the molecular frame, for all parent molecules the transition dipole moments $\boldsymbol{\mu}_i$ are well defined by the polar coordinates (χ_i,φ_i) with respect to the recoil velocity **v** and the molecular principal axis **d**. This approximation implies a one-to-one correspondence between the fixed molecular geometry (defined by **d** and $\boldsymbol{\mu}_i$) and **v** so that all the parent molecules are identical in the molecular frame and differ only with respect to each other by their orientation in the laboratory frame (i.e., the angles between **v** and the $\boldsymbol{\mu}_i$ with respect to photodissociation and probe laser polarization directions). Therefore, the photofragment angular distribution can be described by the product of the absorption probability with the photofragment detection probability, integrated over all molecular geometries that contribute to a particular product velocity **v**. We justify the use of this model, beyond the intuitive picture it presents and the previous success of the similar approach by Rakitzis and Zare for diatomic molecules, by the fact that the full-quantum treatment for the rotational depolarization factors of the photofragment angular momentum distributions[77] can be derived exactly using the treatment presented here. Therefore, we believe that this work represents an interesting limiting case with which future, more exact treatments can be compared.

Figure 1 shows a molecular plane of the molecule, which contains **d** and $\boldsymbol{\mu}_i$; however, note that the recoil frame is defined instead by the **v**-**d** plane. The **v**-**d** and the $\boldsymbol{\mu}_i$-**d** planes may not be parallel for various reasons, including (a) the photofragment M recoils nonaxially out of the $\boldsymbol{\mu}_i$-**d** plane and (b) the M-N bond originally points out of the $\boldsymbol{\mu}_i$-**d** plane, and thus **v** remains out of this plane, even for axial recoil dissociation. We are considering the case where the vectors **v**, **d**, and $\boldsymbol{\mu}_i$ are well described in the recoil frame by the polar angles (χ_i,φ_i). It should be noted that the point of the treatment here is to calculate the consequences that arise from this geometrical relationship.

The angular momentum distribution of an ensemble of angular momenta **J** (originating from photodissociation via the state i) can be described by the complete set of polarization parameters, $a_q^k(i)$. The photofragments M are detected with in a manner sensitive to both the $a_q^k(i)$ and the velocity

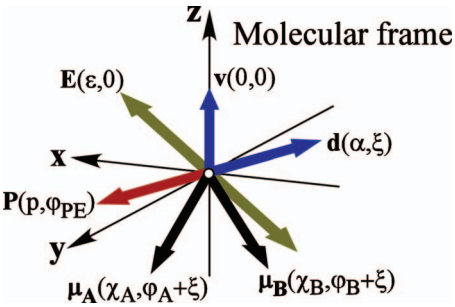

FIG. 2. Polar coordinates of the dynamical vectors ($\mathbf{v}$, $\boldsymbol{\mu}_A$, $\boldsymbol{\mu}_B$, and $\mathbf{d}$), the photolysis ($\mathbf{E}$), and probe ($\mathbf{P}$) polarization directions in the molecular frame, for the photodissociation of asymmetric top molecules. Vectors are given in terms of polar angles (θ,φ), where θ is the polar angle (with $\mathbf{v}$) and φ is the azimuthal angle with respect to the plane defined by $\mathbf{E}$ and $\mathbf{v}$.

of the photofragments, such as REMPI or laser-induced fluorescence (LIF). The polarization dependent detection probability $I[a_q^k(i)]$ can be expressed by the expansion

$$I[a_q^k(i)] = 1 + \sum_{k=1}^{2J} s_k \sum_{q=-k}^{k} a_q^k(i) C_q^k(p, \varphi_{dP}), \tag{3}$$

where the $C_q^k(\theta,\varphi)$ are reduced spherical harmonics,[13] p is the angle between $\mathbf{v}$ and the probe laser polarization direction $\mathbf{P}$, φ_{dP} is the azimuthal angle between $\mathbf{d}$ and $\mathbf{P}$ about $\mathbf{v}$ (see Fig. 2), and the s_k are the detection sensitivity factors of the $a_q^k(i)$ (expressions for the s_k are given below for 2+1 REMPI). This molecular frame detection probability is completely general and is independent of the photodissociation mechanism. The aim of this paper is to derive the geometrical constraints imposed on the detection sensitivity of each of the $a_q^k(i)$ parameters by the asymptotic geometrical relationship between the dynamical vectors $\mathbf{d}$, $\boldsymbol{\mu}_i$, and $\mathbf{v}$.

The total detection probability $I[a_q^k(i)]$, for the URD approximation, is given by the product of absorption and detection probabilities, $|\boldsymbol{\mu}_i \cdot \mathbf{E}|^2$ and $D[a_q^k(i)]$, integrated over all possible molecular geometries which yield photofragments M parallel to $\mathbf{v}$,

$$I[a_q^k(i)] = \frac{1}{2\pi}\int_0^{2\pi} 3|\boldsymbol{\mu}_i \cdot \mathbf{E}|^2 D[a_q^k(i)] d\xi, \tag{4}$$

where ξ is the azimuthal angle of $\mathbf{d}$ about $\mathbf{v}$. The factor of 3 has been included for the normalization of subsequent equations. Expressing $|\boldsymbol{\mu}_i \cdot \mathbf{E}|^2$ in terms of the Legendre polynomials, Eq. (4) can be written as

$$I[a_q^k(i)] = \frac{1}{2\pi}\int_0^{2\pi} [1 + 2P_2(\cos\,\theta_{\mu_i E})] \times \left[1 + \sum_{k=1}^{2J} s_k \sum_{q=-k}^{k} a_q^k C_q^k(p) e^{iq\varphi_{dP}}\right] d\xi. \tag{5}$$

The projection $\cos\,\theta_{\mu_i E}$ can be expressed in terms of the molecular frame angles by

$$\cos\,\theta_{\mu_i E} = \cos\,\chi_i \cos\,\varepsilon + \sin\,\chi_i \sin\,\varepsilon \cos(\varphi_i + \xi). \tag{6}$$

The summation over the a_q^k parameters can be written to be purely real using the expression

$$a_q^k C_q^k(\theta) e^{iq\varphi} + a_{-q}^k C_{-q}^k(\theta) e^{-iq\varphi} = 2C_q^k(\theta)(\mathrm{Re}[a_q^k]\cos\,q\varphi + \mathrm{Im}[a_q^k]\sin\,q\varphi). \tag{7}$$

Finally, applying the spherical harmonic addition theorem, inserting Eqs. (6) and (7), and using $\varphi_{dP} = \xi - \varphi_{PE}$, Eq. (5) can be written as

$$I[a_q^k(i)] = \frac{1}{2\pi}\int_0^{2\pi} [1 + 2C_0^2(\chi_i)C_0^2(\varepsilon) + 4C_1^2(\chi_i)C_1^2(\varepsilon) \times \cos(\varphi_i + \xi) + 4C_2^2(\chi_i)C_2^2(\varepsilon)\cos\,2(\varphi_i + \xi)] \times \left[1 + \sum_{k=1}^{2J} s_k \sum_{q=-k}^{k} (2 - \delta_{q0}) C_q^k(p)(\mathrm{Re}[a_q^k(i)] \times \cos\,q(\xi - \varphi_{PE}) + \mathrm{Im}[a_q^k(i)]\sin\,q(\xi - \varphi_{PE}))\right] d\xi. \tag{8}$$

Evaluating Eq. (8), we obtain the general recoil-frame detection probability

$$\begin{aligned} I[a_q^k(i)] = {} & [1 + 2C_0^2(\chi_i)C_0^2(\varepsilon)]\left[1 + \sum_{k=1}^{2J} s_k a_0^k(i) C_0^k(p)\right] \\ & + 4\sum_{k=1}^{2J} s_k\, \mathrm{Re}[a_1^k(i)] C_1^2(\chi_i) C_1^2(\varepsilon) C_1^k(p) \cos(\varphi_i + \varphi_{PE}) \\ & - 4\sum_{k=1}^{2J} s_k\, \mathrm{Im}[a_1^k(i)] C_1^2(\chi_i) C_1^2(\varepsilon) C_1^k(p) \sin(\varphi_i + \varphi_{PE}) \\ & + 4\sum_{k=1}^{2J} s_k\, \mathrm{Re}[a_2^k(i)] C_2^2(\chi_i) C_2^2(\varepsilon) C_2^k(p) \cos\,2(\varphi_i + \varphi_{PE}) \\ & - 4\sum_{k=1}^{2J} s_k\, \mathrm{Im}[a_2^k(i)] C_2^2(\chi_i) C_2^2(\varepsilon) C_2^k(p) \sin\,2(\varphi_i + \varphi_{PE}), \end{aligned} \tag{9a}$$

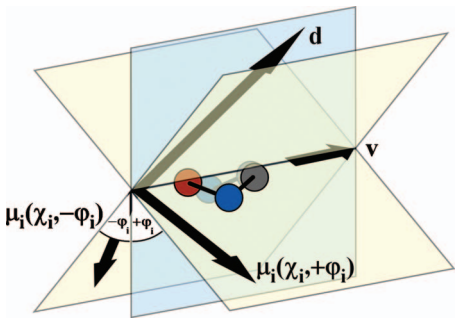

FIG. 3. The azimuthal angles of $\boldsymbol{\mu}_i$ and $\mathbf{d}$ about $\mathbf{v}$: For a nonchiral, asymmetric top molecule, there are two, equally likely, molecular geometries that share $\mathbf{v}$ and $\mathbf{d}$, but not $\boldsymbol{\mu}_i$, as they have opposite signs for the azimuthal angle between $\boldsymbol{\mu}_i$ and $\mathbf{d}$ ($+\varphi_i$ and $-\varphi_i$).

which can be expressed compactly to show the symmetry of the expression as

$$I[a_q^k(i)] = \left[1 + 2C_0^2(\chi_i)C_0^2(\varepsilon) + \sum_{k=1}^{2J} s_k a_0^k(i) C_0^k(p) \right] + 2\sum_{k=1}^{2J} s_k \sum_{q=-2}^{2} a_q^k(i) C_q^2(\chi_i) C_q^2(\varepsilon) C_{-q}^k(p) e^{iq(\varphi_i+\varphi_{PE})}. \tag{9b}$$

Equation (9) is a general expression describing the photofragment polarization from photodissociation via a single excited state i; it contains all the terms for the description of the photodissociation of chiral molecules, i.e., some of the terms do not have inversion symmetry[82] unlike the distributions of nonchiral molecules.[3] For convenience, Eq. (9a) is expressed in a longer form, necessary for all the terms to be explicitly real.

We next consider the photodissociation of an ensemble of nonchiral molecules or of a racemic mixture of chiral molecules. Figure 3 shows the recoil frame (defined by **v** and the **v**-**d** plane) as our choice for the description of the photofragment polarization: For nonchiral molecules, there are two distinct geometries of molecules which share **v** and **d**, but not $\boldsymbol{\mu}_i$ (i.e., those with $+\varphi_i$ and $-\varphi_i$, which are equally likely). Therefore, the detection probability must be invariant under the transformation $\varphi_i \rightarrow -\varphi_i$ so that $\langle \sin q\varphi_i \rangle = 0$. In addition, the photofragment angular momentum distribution should have reflection symmetry through the **v**-**d** plane; as the probe polarization direction is a pseudovector, this reflection constrains the angular momentum distribution to be invariant under the transformations $p \rightarrow \pi - p$ and $\varphi_{PE} \rightarrow \pi - \varphi_{PE}$. Averaging Eq. (9) over this reflection, we obtain the recoil-frame detection probability for photofragments from the photodissociation of nonchiral molecules,

$$I[a_q^k(i)] = [1 + 2C_0^2(\chi_i)C_0^2(\varepsilon)]\left[1 + \sum_{\text{even } k}^{2J} s_k a_0^k(i) C_0^k(p) \right] + 4\sum_{\text{even } k}^{2J} s_k \,\text{Re}[a_1^k(i)] C_1^2(\chi_i) C_1^2(\varepsilon) C_1^k(p) \cos\varphi_i \cos\varphi_{PE} - 4\sum_{\text{odd } k}^{2J} s_k \,\text{Im}[a_1^k(i)] C_1^2(\chi_i) C_1^2(\varepsilon) C_1^k(p) \cos\varphi_i \sin\varphi_{PE} + 4\sum_{k}^{2J} s_k \,\text{Re}[a_2^k(i)] C_2^2(\chi_i) C_2^2(\varepsilon) C_2^k(p) \cos 2\varphi_i \cos 2\varphi_{PE}, \tag{10}$$

where the summations over k begin at 2, except for the third summation over odd k which begins at 1. In contrast to Eq. (9), notice that no terms in Eq. (10) violate inversion symmetry. In future work, we will show how sensitivity to some of these parameters can be attained using circularly polarized photolysis light [the $a_0^k(i)$ with odd k, the $\text{Re}[a_1^k(i)]$ with odd k, and the $\text{Im}[a_1^k(i)]$ with even k]; the other parameters that vanished from Eq. (9) can only be observed from the photodissociation of chiral molecules.

Equations (9) and (10) are important results, as they show how the sensitivity to the $a_q^k(i)$ parameters depends on the angles χ_i and φ_i (the polar angles of $\boldsymbol{\mu}_i$ in the recoil frame). The sensitivity dependence is best seen by renormalizing Eq. (10) to the photofragment population for a given scattering angle γ, which is $[1+2C_0^2(\chi_i)C_0^2(\varepsilon)]$. Then, we see that the sensitivity to the $a_q^k(i)$ parameters with $q=0$ is independent of χ_i and φ_i whereas the sensitivity to the $a_q^k(i)$ parameters with $q=1$ or $q=2$ is proportional to $C_q^2(\chi_i)C_q^2(\varepsilon)\cos q\varphi_i / [1+2C_0^2(\chi_i)C_0^2(\varepsilon)]$; thus we see that the sensitivity to the $a_q^k(i)$ parameters is very small for $\chi_i \approx 0°$ or 90° for $q=1$, or for $\chi_i \approx 0°$ for $q=2$ [as expected for a transition that is parallel ($\chi_i=0°$) or perpendicular ($\chi_i=90°$)]. These results are strongly analogous to the sensitivities to the $A_q^{(k)stf}$ in bimolecular scattering in photoloc experiments,[83] as the methods of derivation have strong similarities.

It is also worth noticing that the sensitivity to each of the $a_q^k(i)$ parameters is proportional to $\cos q\varphi_i$. For $q=0$, there is, of course, no detection sensitivity dependence on φ_i; however, for $q=1$ and $q=2$ the sensitivity dependences are $\cos\varphi_i$ and $\cos 2\varphi_i$, respectively. Note that φ_i is the azimuthal angle between $\boldsymbol{\mu}_i$ and **d** about **v**, and that this angle can be strongly determined by nonaxial recoil dynamics. The sensitivity to $q=1$ parameters vanishes at $|\varphi_i|=90°$ (see Fig. 4), and the sensitivity to $q=2$ parameters vanishes at $|\varphi_i|=45°$; therefore the measurement of large values of $q=1$ or $q=2$ parameters sets constraints on the value of φ_i and gives information on the symmetry of the excited state i and on the directionality of nonaxial recoil of the photofragments. For example, let us consider the photodissociation of a triatomic molecule, such as OCS or NO_2, via the A'' excited state for which $\boldsymbol{\mu}_{A''}$ is perpendicular to the molecular plane at the time of absorption of the photodissociating photon. If the photofragment recoil velocity remains in this plane (such that $\boldsymbol{\mu}_{A''}$ is perpendicular to the **v**-**d** plane), then $|\varphi_{A''}|=90°$, in which case the sensitivity to the $q=1$ $a_q^k(A'')$ parameters vanishes (as a reminder we note that these $q=1$ parameters are the $\text{Re}[a_1^k]$ for even k and the $\text{Im}[a_1^k]$ for odd k). However, large values of $q=1$ parameters have been measured from the photodissociation of OCS.[56–59] In these cases, we can conclude that the measured $q=1$ a_q^k parameters are *not* being produced by excitation to the A'' state, followed by in-plane recoil. Possible explanations include out-of-plane recoil dynamics (following A'' excitation) or in-plane recoil dynamics (following A' excitation); contributions from the interference of multiple excited states are possible and discussed below.

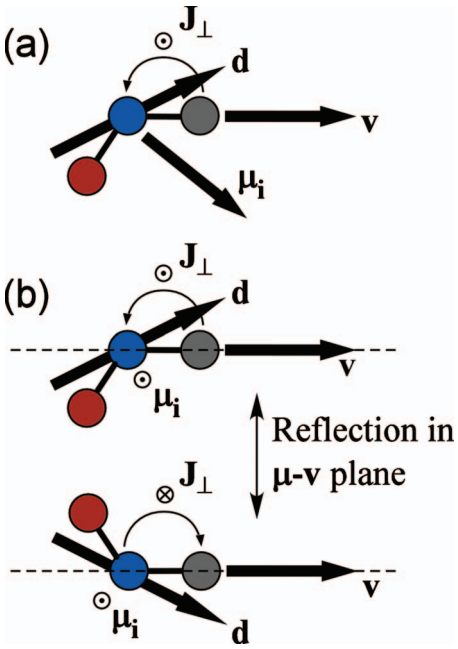

FIG. 4. (a) Photodissociation of a triatomic molecule is shown with **v**, **d**, and $\boldsymbol{\mu}_i$ all in the same plane. Reflection through the **v**-$\boldsymbol{\mu}_i$ plane leaves the molecule (and **J** distribution) unchanged. (b) Photodissociation of a triatomic molecule is now shown with $\boldsymbol{\mu}_i$ perpendicular to the **v**-**d** plane. In this case, reflection through the **v**-$\boldsymbol{\mu}_i$ plane produces a photodissociating molecule that shares **v** and $\boldsymbol{\mu}_i$, but a different **d** and an inverted $\mathbf{J}_\perp$. The averaging of these two, equally likely, molecular geometries (for isotropic parent molecules) causes the $q=1$ parameters to vanish.

B. Multiple surface dissociation

Next, we consider coherent and incoherent effects from photodissociation via two dissociative states, A and B, with transition dipole moments $\boldsymbol{\mu}_A$ and $\boldsymbol{\mu}_B$, which have molecular frame coordinates (χ_A,φ_A) and (χ_B,φ_B), respectively (see Fig. 2). The total transition dipole moment $\boldsymbol{\mu}_T$ is expressed as a weighted average of $\boldsymbol{\mu}_A$ and $\boldsymbol{\mu}_B$, given by $\boldsymbol{\mu}_T=c_A\boldsymbol{\mu}_A+c_B\boldsymbol{\mu}_B$. The product of the absorption probability $|\boldsymbol{\mu}_T\cdot\mathbf{E}|^2$ with the detection probability $D[a_q^k(s)]$, integrated over all molecular geometries, is given by

$$I[a_q^k]=\frac{3}{2\pi}\int_0^{2\pi}[c_A^2|\boldsymbol{\mu}_A\cdot\mathbf{E}|^2D(a_q^k(A))+c_B^2|\boldsymbol{\mu}_B\cdot\mathbf{E}|^2D(a_q^k(B))+2c_Ac_B(\boldsymbol{\mu}_A\cdot\mathbf{E})\times(\boldsymbol{\mu}_B\cdot\mathbf{E})D(a_q^k(A,B))]d\xi. \tag{11}$$

We note that since both the A and B states are excited with linearly polarized light, the phase difference is initially 0 so that we can choose c_A and c_B to be both real.

Equation (11) is evaluated, following similar steps as those shown from Eqs. (5)–(8), (9a), (9b), and (10). The resulting detection probability expression in the recoil frame, for linearly polarized photolysis light, and for nonchiral molecules, is then given by

$$\begin{aligned}I(a_q^k)=c_A^2I[a_q^k(A)]+c_B^2I[a_q^k(B)]+2c_Ac_B\Bigg\{&[\cos\theta_{AB}+(3\cos\chi_A\cos\chi_B-\cos\theta_{AB})P_2(\cos\varepsilon)]\Bigg(\sum_{k\ \text{even}}^{2J}a_0^k(A,B)C_0^k(p)\Bigg)\\&+[3(\sin\chi_A\cos\chi_B\cos\varphi_A+\sin\chi_B\cos\chi_A\cos\varphi_B)\sin\varepsilon\cos\varepsilon]\Bigg(\sum_{\text{even}\ k}^{2J}s_k\,\mathrm{Re}[a_1^k(A,B)]C_1^k(p)\cos\varphi_{PE}\\&-\sum_{\text{odd}\ k}^{2J}s_k\,\mathrm{Im}[a_1^k(A,B)]C_1^k(p)\sin\varphi_{PE}\Bigg)+\left[\frac{3}{2}\sin\chi_A\sin\chi_B\cos(\varphi_A+\varphi_B)\sin^2\varepsilon\right]\\&\times\Bigg(\sum_{\text{even}\ k}^{2J}s_k\,\mathrm{Re}[a_2^k(A,B)]C_2^k(p)\cos2\varphi_{PE}-\sum_{\text{odd}\ k}^{2J}s_k\,\mathrm{Im}[a_2^k(A,B)]C_2^k(p)\sin2\varphi_{PE}\Bigg)\Bigg\},\end{aligned} \tag{12}$$

where $I[a_q^k(A)]$ and $I[a_q^k(B)]$ are given by Eq. (10) with $i=A$ and B, respectively, $c_A^2+c_B^2=1$, and θ_{AB} is the angle between the dipole moments $\boldsymbol{\mu}_A$ and $\boldsymbol{\mu}_B$, with molecular frame coordinates (χ_A,φ_A) and (χ_B,φ_B), respectively, and is given by

$$\cos\theta_{AB}=\cos\chi_A\cos\chi_B+\sin\chi_A\sin\chi_B\cos(\varphi_A-\varphi_B). \tag{13}$$

We return to the example of the photodissociation of a triatomic molecule, such as OCS, where we discussed the geometric dependence of the $q=1$ parameters arising from single-surface photodissociation. Here we discuss components of the $q=1$ parameters that arise from dissociation following the coherent excitation of the A and B dissociative states; we see from Eq. (12) that the $q=1$ parameters are proportional to the geometric factor $(\sin\chi_A\cos\chi_B\cos\varphi_A+\sin\chi_B\cos\chi_A\cos\varphi_B)$. Let us consider excitation via the A'' state, for which $\boldsymbol{\mu}_{A''}$ is perpendicular to the OCS plane at the time of absorption of the photodissociating photon, and an A' state (for which $\boldsymbol{\mu}_{A'}$ is initially parallel to the OCS plane).

If we assume that the recoil **v** remains in this molecular plane, then the $\boldsymbol{\mu}_{A''}$ and $\boldsymbol{\mu}_{A'}$ coordinates are given by ($\chi_{A''}=90°$, $\varphi_{A''}=90°$) and ($\chi_{A'}=\chi$, $\varphi_{A'}=0°$), respectively. For these values, the sensitivity factor to the $a_q^k(A,B)$ parameters vanishes: $(\sin\chi_{A''}\cos\chi_{A'}\cos\varphi_{A''}+\sin\chi_{A'}\cos\chi_{A''}\cos\varphi_{A'})=0$. This is a very interesting result, as it says that $q=1$ parameters cannot arise from A'' state excitation, either directly (single-state excitation) or via interference with another state (two-state excitation), *if* the photofragment recoil **v** remains in the molecular plane.

C. General description of photofragment polarization

Comparing the single-state dissociation expression of Eq. (10) with the two-state dissociation expression of Eq. (12), we see both can be expressed conveniently into the general form,

$$I=1+c\beta C_0^2(\varepsilon)+s_1\,\mathrm{Im}[A_1^1]C_1^1(p)C_1^2(\varepsilon)\sin\varphi_{PE}+s_2\{A_0^2(\mathrm{iso})C_0^2(p)+A_0^2(\mathrm{aniso})C_0^2(p)C_0^2(\varepsilon)+\mathrm{Re}[A_1^2]C_1^2(p)C_1^2(\varepsilon)\cos\varphi_{PE}+\mathrm{Re}[A_2^2]C_2^2(p)C_2^2(\varepsilon)\cos 2\varphi_{PE}\}+s_3\{\mathrm{Im}[A_1^3]C_1^3(p)C_1^2(\varepsilon)\sin\varphi_{PE}+\mathrm{Re}[A_2^3]C_2^3(p)C_2^2(\varepsilon)\cos 2\varphi_{PE}\}+s_4\{A_0^4(\mathrm{iso})C_0^4(p)+A_0^4(\mathrm{aniso})C_0^4(p)C_0^2(\varepsilon)+\mathrm{Re}[A_1^4]C_1^4(p)C_1^2(\varepsilon)\cos\varphi_{PE}+\mathrm{Re}[A_2^4]C_2^4(p)C_2^2(\varepsilon)\cos 2\varphi_{PE}\}. \tag{14}$$

We emphasize that the A_q^k parameters are polarization-parameter coefficients in the general molecule-frame expansion of Eq. (14). Although they can have a distinct physical interpretation (within limits of approximations such as the URD approximation), they are not multipole moments of the photofragment angular momentum distribution. Note that the terms in Eq. (14) form a complete basis (up to $k=4$) for the description of experimental photofragment polarization signals for the one-photon photodissociation of molecules of any achiral symmetry, using a detection scheme that is sensitive to A_q^k parameters up to $k=4$ (such as 2+n REMPI or LIF, where the second step is not polarization sensitive). This A_q^k parameter expansion is functionally equivalent (although in somewhat different form) to the bipolar moment expansion used by Dixon,[3] in that both expansions form a complete basis set. Below, however, we give interpretations of the A_q^k in terms of molecular frame geometric factors and dynamics parameters. For simplicity, in Eq. (14), the summation over k has been evaluated explicitly up to $k=4$ (terms higher than $k=4$ have never been yet measured); however generalization to higher k is straightforward. Notice that the $\mathrm{Re}[A_q^k]$ with odd k and the $\mathrm{Im}[A_q^k]$ with even k are absent here with linearly polarized photolysis light; they are present only for circularly polarized photolysis light or for chiral molecules.

The interpretation of the measured A_q^k parameters is given for single-state and multiple-state dissociations (within the URD approximation).

(a) For the photodissociation of nonchiral molecules (not limited by axial recoil) via a single dissociative state, β and the A_q^k are given by comparing Eqs. (10) and (14),

$$\beta=2C_0^2(\chi_i), \tag{15a}$$

$$A_0^k(\mathrm{iso})=a_0^k(i), \tag{15b}$$

$$A_0^k(\mathrm{aniso})=2C_0^2(\chi_i)a_0^k(i), \tag{15c}$$

$$A_q^k=(-1)^{kq}4gC_q^2(\chi_i)\cos q\varphi_i a_q^k(i). \tag{15d}$$

(b) For photodissociation via two dissociative states A and B, β and the A_q^k parameters are given by comparing Eqs. (12) and (14) (note that $c_A^2+c_B^2=1$),

$$\beta=2[c_A^2C_0^2(\chi_A)+c_B^2C_0^2(\chi_B)], \tag{16a}$$

$$A_0^k(\mathrm{iso})=c_A^2a_0^k(A)+c_B^2a_0^k(B)+2c_Ac_B\cos\theta_{AB}\,a_0^k(A,B), \tag{16b}$$

$$A_0^k(\mathrm{aniso})=2[c_A^2C_0^2(\chi_A)a_0^k(A)+c_B^2C_0^2(\chi_B)a_0^k(B)+c_Ac_B(3\cos\chi_A\cos\chi_B-\cos\theta_{AB})a_0^k(A,B)], \tag{16c}$$

$$A_1^k=(-1)^k2g\sqrt{6}[c_A^2\sin\chi_A\cos\chi_A\cos\varphi_Aa_1^k(A)+c_B^2\sin\chi_B\cos\chi_B\cos\varphi_Ba_1^k(B)-c_Ac_B(\sin\chi_A\cos\chi_B\cos\varphi_A+\sin\chi_B\cos\chi_A\cos\varphi_B)a_1^k(A,B)], \tag{16d}$$

$$\mathrm{Re}[A_2^k]=g\sqrt{6}[c_A^2\sin^2\chi_A\cos 2\varphi_A\,\mathrm{Re}[a_2^k(A)]+c_B^2\sin^2\chi_B\cos 2\varphi_B\,\mathrm{Re}[a_2^k(B)]+2c_Ac_B\sin\chi_A\sin\chi_B\cos(\varphi_A+\varphi_B)\,\mathrm{Re}[a_2^k(A,B)]]. \tag{16e}$$

For diatomic, spherical top, and symmetric top molecules (in the axial recoil limit), $g=2$, $\varphi_i=0$, and $\chi_i=0$ or $\pi/2$ [then Eq. (16) reduces to the cases given in Refs. 12 and 84]. For asymmetric top molecules, χ_i and φ_i can take on any value, and $g=1$; in this case, the reduction in the A_q^k by $\frac{1}{2}\cos q\varphi_i$ arises from the fact that the angle between the $\boldsymbol{\mu}$-**v** and **v**-**E** planes can take on all the values from 0 to 2π, whereas for the axial recoil photodissociation of diatomic, symmetric top, or spherical top molecules the $\boldsymbol{\mu}$-**v** and **v**-**E** planes are always parallel.

We can see that if the ratio of $A_0^k(\mathrm{aniso})/A_0^k(\mathrm{iso})$ is given by β, as is the case for Eqs. (15b) and (15c), then the data are

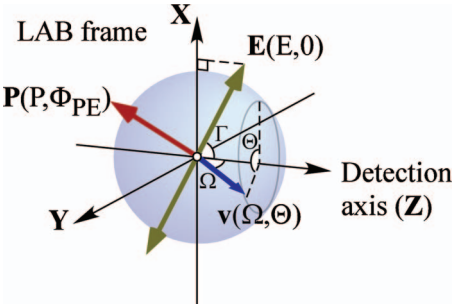

FIG. 5. Polar coordinates of the photofragment recoil **v**, the photolysis (**E**), and probe (**P**) polarization directions in the laboratory frame. The detection axis defines Z (e.g., Z is the direction of the probe beam in Doppler spectroscopy, or Z points toward the microchannel plate detector in TOF mass spectrometry or velocity map imaging). Vectors are given in terms of polar coordinates (θ,φ) where θ is the polar angle (angle from the Z axis) and φ is the azimuthal angle with respect to the plane defined by **E** and Z. In this diagram, the photolysis vector **E** is limited to linear polarization and represents the axis of the linear polarization of the light (i.e., the electric field vector). Note that for linearly polarized probe light, the vector **P** is defined by the axis of the linear polarization (the electric field vector), whereas for circularly polarized probe light **P** is defined as the direction of the circularly polarized beam.

consistent with a single dissociative surface [as is the case for Eqs. (16b) and (16c), if either c_A or c_B are 0]. This test can be used to see whether a single surface suffices to explain measured photofragment angular momentum distributions.

We note that the parameters $a_q^k(A,B)$, as interference terms, are proportional to $e^{i\Delta\Phi_{AB}}$, where $\Delta\Phi_{AB}$ is the asymptotic phase shift between the dissociating wavefunctions associated with states A and B. Therefore, the $\mathrm{Re}[a_q^k(A,B)]$ parameters are proportional to $\cos\Delta\Phi_{AB}$ and the $\mathrm{Im}[a_q^k(A,B)]$ parameters are proportional to $\sin\Delta\Phi_{AB}$.

D. Transformation from the molecular to the laboratory frame

Figure 5 shows the laboratory-frame coordinates of the recoil velocity **v**, with respect to the photolysis and probe laser polarization directions **E** and **P**, respectively. The Z-axis is parallel to the detection axis [e.g., the time-of-flight (TOF) axis of a mass spectrometer], and the Y-axis is defined by $\mathbf{Z}\times\mathbf{E}$ (see Fig. 5). The expressions for the polar angles in the molecular frame, ε and p, in terms of the laboratory-frame angles are given by[8,83]

$$\cos\varepsilon = \cos\Omega\cos E + \sin\Omega\sin E\cos\Theta, \tag{17a}$$

$$\cos p = \cos\Omega\cos P + \sin\Omega\sin P\cos(\Theta - \Phi_{PE}), \tag{17b}$$

and expressions for trigonometric functions of the molecular frame azimuthal angles, $\cos\varphi_{PE}$ and $\sin\varphi_{PE}$, in terms of the laboratory-frame angles are given by

$$\begin{aligned}\cos\varphi_{PE} = \{&\sin^2\Omega\cos E\cos P + \sin E\sin P\cos\Phi_{PE}\\ &-\sin\Omega\cos\Omega[\sin P\cos E\cos(\Phi-\Theta)\\ &+\sin E\cos P\cos\Theta] - \sin^2\Omega\sin E\sin P\\ &\times\cos(\Phi-\Theta)\cos\Theta\}/(\sin\varepsilon\sin p),\end{aligned} \tag{18a}$$

$$\begin{aligned}\sin\varphi_{PE} = \{&\cos\Omega\sin E\sin P\sin\Phi_{PE}\\ &-\sin\Omega[\sin P\cos E\sin(\Phi_{PE}-\Theta)\\ &+\sin E\cos P\sin\Theta]\}/(\sin\varepsilon\sin p).\end{aligned} \tag{18b}$$

Inserting Eqs. (17) and (18) in the molecular frame expressions, such as Eq. (14), gives the full three-dimensional laboratory-frame photofragment angular momentum distribution. Methods for collapsing the full three-dimensional distribution to projections in one dimension (such as TOF or Doppler profiles) or two dimensions (such as ion imaging) are given in Secs. 3.1 and 3.2 in Ref. 8. Calculations of the angular momentum distribution in the laboratory frame are performed in Appendix B, which show how Eqs. (14), (17), and (18) can be used straightforwardly.

E. Detection sensitivity factors and a_0^k physical ranges

The experimental sensitivity to the A_q^k (ignoring geometrical factors) is determined by the nature of the photofragment detection transition.[85,86] The most commonly used detection scheme is 2+1 REMPI.[87] For this case, the A_q^k detection sensitivity factors s_k are given by

$$s_k = P_k\frac{[J(J+1)]^{k/2}\sqrt{2k+1}\sqrt{2J+1}}{c(k)\langle J||J^{(k)}||J\rangle}, \tag{19}$$

where the reduced matrix elements $\langle J||J^{(k)}||J\rangle$ are given in Application 13 in Ref. 13, the $c(k)$ are given in Ref. 14, and expressions for the P_k are given in Ref. 88. For convenience, Eq. (19) has been evaluated for $k=1-4$ and for all ΔJ ranging from -2 to $+2$ ($\Delta J = J' - J$, where J' and J are the intermediate and ground state angular momentum quantum numbers of the photofragment, respectively). These explicit expressions for the s_k are shown in Table I, for both linearly and circularly polarized probe light. For the case of the $\Delta J = 0$ transition with linearly polarized probe light, the value of the s_k is not generally correct, as it is necessary to sum over the virtual states of the two-photon transition;[88] therefore, these particular transitions should be used only if the value of the s_k has been calculated specifically to the case in hand, or calibrated experimentally. We suggest avoiding these cases, if possible.

In the high-J limit, the values of the a_0^k parameters are expressed straightforwardly in terms of the projection of J along the z axis, which is $\cos\theta$ (proportional to the M quantum number). In terms of the expectation value of the kth Legendre polynomial,

$$a_0^k = (1+\delta_{k2})\langle P_k(\cos\theta)\rangle, \tag{20}$$

where $\cos\theta = M/\sqrt{J(J+1)}$ (notice that there is an extra prefactor of 2 for $k=2$ only). However, for low values of J, the values of the a_0^k depart from those predicted by Eq. (20). The relationship between the density matrix elements $\rho_{MM'}$ and a_q^k is given elsewhere,[13,14] from which we derive the exact relation between the a_0^k and $\cos\theta$,

$$a_0^1 = \langle P_1(\cos\theta)\rangle, \tag{21a}$$

$$a_0^2 = 2\langle P_2(\cos\theta)\rangle, \tag{21b}$$

TABLE I. The detection sensitivity factors s_k for (2+n) REMPI, where the detection step is saturated, tabulated for $k=1$, 2, 3, and 4, and for $\Delta J=-2,-1,0,+1$, and +2. J is the photofragment angular momentum, $\Delta J=J'-J$, where J' is the angular momentum of the intermediate state of the REMPI transition, and λ denotes the polarization of the probe laser ($\lambda=0$ for linearly polarized light, and $\lambda=\pm 1$ for $\sigma_{\pm}$ circularly polarized probe light). The s_k are calculated using Eq. (19). The $\Delta J=0$ transitions with linearly polarized probe light ($\lambda=0$) should be used with care (see text for details).

ΔJ	$s_1(J,\Delta J,\lambda)$	$s_2(J,\Delta J,\lambda)$	$s_3(J,\Delta J,\lambda)$	$s_4(J,\Delta J,\lambda)$
−2	$-2\lambda\frac{(J+1)}{\sqrt{J(J+1)}}$	$-\frac{10}{7}\frac{(J+1)}{(2J-1)}(-1)^{\lambda}$	$-\lambda\frac{(J+1)\sqrt{J(J+1)}}{(J-1)(2J-1)}$	$+\frac{12}{7}\frac{J(J+1)^2(6)^{-\lvert\lambda\rvert}}{(J-1)(2J-1)(2J-3)}$
−1	$-\lambda\frac{(J+3)}{\sqrt{J(J+1)}}$	$+\frac{5}{7}\frac{(J-5)}{(2J-1)}(-1)^{\lambda}$	$+2\lambda\frac{(J-2)\sqrt{J(J+1)}}{(J-1)(2J-1)}$	$-\frac{24}{7}\frac{J(J+1)(6)^{-\lvert\lambda\rvert}}{(J-1)(2J-1)}$
0	$-3\lambda\frac{1}{\sqrt{J(J+1)}}$	$-\frac{5}{7}\frac{(2J-3)(2J+5)}{(2J-1)(2J+3)}(-1)^{\lambda}$	$+12\lambda\frac{\sqrt{J(J+1)}}{(2J-1)(2J+3)}$	$+\frac{72}{7}\frac{J(J+1)(6)^{-\lvert\lambda\rvert}}{(2J-1)(2J+3)}$
+1	$+\lambda\frac{(J-2)}{\sqrt{J(J+1)}}$	$+\frac{5}{7}\frac{(J+6)}{(2J+3)}(-1)^{\lambda}$	$-2\lambda\frac{(J+3)\sqrt{J(J+1)}}{(J+2)(2J+3)}$	$-\frac{24}{7}\frac{J(J+1)(6)^{-\lvert\lambda\rvert}}{(J+2)(2J+3)}$
+2	$+\lambda\frac{2J}{\sqrt{J(J+1)}}$	$-\frac{10}{7}\frac{J}{(2J+3)}(-1)^{\lambda}$	$+\lambda\frac{J\sqrt{J(J+1)}}{(J+2)(2J+3)}$	$+\frac{12}{7}\frac{J^2(J+1)(6)^{-\lvert\lambda\rvert}}{(J+2)(2J+3)(2J+5)}$

$$a_0^3=\langle P_3(\cos\theta)\rangle+\frac{\frac{1}{2}\langle\cos\theta\rangle}{J(J+1)}, \tag{21c}$$

$$a_0^4=\langle P_4(\cos\theta)\rangle+\frac{\frac{25}{8}\langle\cos^2\theta\rangle-\frac{3}{4}}{J(J+1)}, \tag{21d}$$

$$a_0^5=\langle P_5(\cos\theta)\rangle+\frac{\frac{45}{8}\langle\cos^3\theta\rangle-\frac{7}{4}\langle\cos\theta\rangle}{J(J+1)}, \tag{21e}$$

$$a_0^6=\langle P_6(\cos\theta)\rangle+\frac{\frac{165}{16}\langle\cos^4\theta\rangle-\frac{321}{112}\langle\cos^2\theta\rangle-\frac{5}{14}}{J(J+1)}. \tag{21f}$$

Equation (21) shows how the values of the a_0^k depart from the high-J limit of Eq. (20), for $k=1-6$. We see that, for $k=1$ and $k=2$, the low and high-J expressions are exactly equal; deviations occur only for $k>2$; notice that as J tends to infinity, Eq. (21) tends to Eq. (20). Equation (21) can be used to determine the physical ranges of the a_0^k as a function of J (see Appendix A).

III. SUMMARY

We presented an expansion [Eq. (14)] which can be used to fit experimental photofragment polarization signals from the photodissociation of molecules with linearly polarized light. It is equivalent to the bipolar moment expansion[3] and is thus completely general (the terms can be expressed as linear combinations of bipolar harmonics, and the coefficients are the A_q^k parameters, which can also be expressed as linear combinations of bipolar moments). However, the A_q^k parameters have a distinct physical interpretation; assuming the URD approximation, the A_q^k are expressed in terms of molecular frame $a_q^k(s)$ parameters (describing the photodissociation dynamics) and also in terms of geometrical factors, which depend on the coordinates of the transition dipole moments in the recoil frame [e.g., the coordinates of $\boldsymbol{\mu}_A$ and $\boldsymbol{\mu}_B$ are given by (χ_A,φ_A) and (χ_B,φ_B)]. We thus separate the geometrical part of the photodissociation process from the dynamical part and detail this separation for the cases of molecular photodissociation via optical excitation to a single electronic state [Eq. (15)], and via coherent excitation to two electronic states [Eq. (16)].

We demonstrate that the condition $A_0^k(\text{aniso})/A_0^k(\text{iso})=\beta$ [where β is the spatial anisotropy parameter given in Eq. (1)] is an indication that the dynamics can be explained by a single dissociative state. We show that $a_q^k(s)$ parameters, with $q=1$, can arise either from single-surface or multiple-surface-interference mechanisms (whereas for diatomic molecules in the axial recoil limit, nonzero values of $a_1^k(p)$ parameters can only arise from multiple-surface interference). We show that the $a_1^k(s)$ can be expressed as sums of terms which are proportional to $\cos\varphi_i$ (where φ_i is the azimuthal angle between $\boldsymbol{\mu}_i$ and $\mathbf{d}$ about $\mathbf{v}$), and therefore the $a_1^k(s)$ parameters are nonzero only for components of the transition dipole moments within the $\mathbf{v}$-$\mathbf{d}$ plane of the recoil frame.

The $a_q^k(s)$ parameter formalism described here has recently been extended to the description of photofragment polarization from single-surface excitation of oriented and aligned molecules.[89] Future work will extend the treatment to circularly polarized photolysis light, to multiple-surface excitation in oriented molecules, to rotating parent molecules, and to the breakdown of the URD approximation.

ACKNOWLEDGMENTS

T.P.R. thanks the EU for support through the European Research Council grant "TRICEPS" (Grant No. 207542) and through the EU-Marie Curie ITN Programme ICONIC (Grant No. PITN-GA-2009-238671).

TABLE II. Tabulation of the values of the a_0^k parameters ($k=1-6$), calculated for $J=3$, and for each M state, and compared to the high-J limit of $P_k(\cos\theta)$, showing the low-J deviation [note that for a_0^1 and a_0^2, there is no deviation between the high- and low-J limits, as shown in Eq. (21)]. Summing over M-states gives 0 for the a_0^k parameters, but not for the $P_k(\cos\theta)$ with even k for $k>2$.

Moment $(J=3,M)$	$a_0^1=P_1(\cos\theta)$	$a_0^2=2P_2(\cos\theta)$	a_0^3	$P_3(\cos\theta)$	a_0^4	$P_4(\cos\theta)$	a_0^5	$P_5(\cos\theta)$	a_0^6	$P_6(\cos\theta)$
−3	−0.866	1.25	−0.361	−0.325	0.156	0.023	0.045	0.223	−0.100	−0.374
−2	−0.577	0	0.361	0.385	−0.365	−0.389	0.090	0.096	0.208	0.222
−1	−0.289	−0.75	0.361	0.373	0.052	0.093	−0.316	−0.347	0.062	0.106
0	0	−1	0	0	0.313	0.375	0	0	−0.342	−0.313
+1	0.289	−0.75	−0.361	−0.373	0.052	0.093	0.316	0.347	0.062	0.106
+2	0.577	0	−0.361	−0.385	−0.365	−0.389	−0.090	−0.096	0.208	0.222
+3	0.866	1.25	0.361	0.325	0.156	0.023	−0.045	−0.223	−0.100	−0.374
Sum	**0**	**0**	**0**	**0**	**0**	**−0.171**	**0**	**0**	**0**	**−0.405**

APPENDIX A: THE a_0^k FOR EACH M STATE OF $J=3$

We show, quantitatively, the difference between Eqs. (20) and (21) in Table II, by tabulating the values of the a_0^k for each M state, for $J=3$, and comparing to the high-J limit of $\langle P_k(\cos\theta)\rangle$. As expected, the deviations become larger with k. Summing over M shows that the low-J expressions sum to 0 (as they should), whereas the high-J values of $\langle P_k(\cos\theta)\rangle$ do not (note that this test is useful for even k only; for odd k the cancellation occurs between values of $+M$ and $-M$). Equation (21) can be used to calculate the physical limits of the a_0^k parameters. For example, for $J=3$, we can inspect Table II to see for which values of M each a_0^k parameter attains its maximal or minimal value, which define the physical limits. In particular, we see that, for $J=3$, the physical ranges of the a_0^k parameters are $0.208\geq a_0^6\geq -0.342$, $0.347\geq a_0^5\geq -0.223$, $0.313\geq a_0^4\geq -0.365$, $0.361\geq a_0^3\geq -0.361$, $1.25\geq a_0^2\geq -1$, and $0.866\geq a_0^1\geq -0.866$.

APPENDIX B: CALCULATION OF LABORATORY-FRAME DISTRIBUTIONS

In this appendix, we present sample calculations of laboratory-frame distributions and consider two cases: (1) Doppler detection using 1+1 LIF and (2) slice imaging using 2+1 REMPI.

1. Doppler detection using 1+1 LIF

We consider the Doppler detection of photofragments using 1+1 LIF (so that k is limited to 2). The photolysis and probe lasers counter-propagate along the Z-axis. For this geometry, both the photolysis and probe laser polarizations are perpendicular to the Z-axis ($E=90°$ and $P=90°$), and we will consider the dependence of the signal on the azimuthal angle between the probe and photolysis laser polarizations about the Z-axis Φ_{PE} [see Fig. 6(a)]. Inserting the values of $E=90°$ and $P=90°$ into Eqs. (17) and (18) we obtain

$$\cos\varepsilon = \sin\Omega\cos\Theta, \tag{B1a}$$

$$\cos p = \sin\Omega\cos(\Theta-\Phi_{PE}), \tag{B1b}$$

$$\cos\varphi_{PE} = \{\cos\Phi_{PE} - \sin^2\Omega\cos(\Phi-\Theta)\cos\Theta\}/(\sin\varepsilon\sin p), \tag{B1c}$$

$$\sin\varphi_{PE} = \cos\Omega\sin\Phi_{PE}/(\sin\varepsilon\sin p). \tag{B1d}$$

These values are inserted into Eq. (14) to give the laboratory intensity distribution. As described by Eq. (10) in Ref. 8, we integrate over Θ from 0 to 2π to give the Doppler intensity distribution,

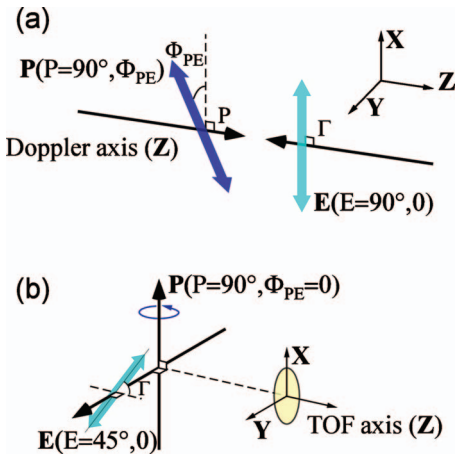

FIG. 6. The experimental geometries, discussed in Appendix B: (a) photolysis and probe lasers counterpropagating along the Z axis (Doppler detection axis), both linearly polarized. Necessarily, both laser linear polarization directions are perpendicular to the Z axis, whereas the azimuthal angle between the polarization directions is Φ_{PE}. (b) The photolysis and probe laser are both perpendicular to each other and to the Z axis (which here is the TOF axis of a slice-imaging detector). The photolysis laser is linearly polarized and set at an angle of 45° to the Z axis. The probe laser is circularly polarized, therefore the polarization direction is parallel to the propagation direction and is perpendicular to Z ($P=90°$) but in the same plane with Z and **E**.

$$I(x) = \left[1 + \frac{s_2}{20}(A_0^2(\text{aniso}) + \text{Re}[A_1^2] + \text{Re}[A_2^2]) \times (1 + 3\cos 2\Phi_{PE})\right] + \left[\frac{1}{2}\beta - \frac{s_2}{2}A_0^2(\text{iso}) + \frac{s_2}{56}(2A_0^2(\text{aniso}) + \text{Re}[A_1^2] - 2\,\text{Re}[A_2^2]) \times (1 - 3\cos 2\Phi_{PE})\right] P_2(x) + \left[\frac{3s_2}{280}(6A_0^2(\text{aniso}) - 4\,\text{Re}[A_1^2] + \text{Re}[A_2^2])(2 + \cos 2\Phi_{PE})\right] P_4(x), \quad \text{(B2)}$$

where $x=\cos\Omega$ is the normalized Doppler shift.[3] When the probe and photolysis laser polarizations are parallel or perpendicular, $\Phi_{PE}=0°$ or 90°, respectively. Notice that Φ_{PE} can be chosen to set the anisotropic components of the alignment to zero for the $P_0(x)$ and the $P_2(x)$ coefficients (at $\cos 2\Phi_{PE}=-1/3$ and $+1/3$, respectively). Methods for inverting polarization parameters from Doppler laboratory distributions are given elsewhere.[3,90–93]

2. Slice imaging using 2+1 REMPI

We consider the slice-imaging of $\text{Cl}(^2P_{3/2})$ photofragments, detected with 2+1 REMPI via the $3s^23p^44p\ ^2P_{1/2} \leftarrow 3s^23p^5\ ^2P_{3/2}$ transition (described by $\Delta J=-1$) with circularly polarized probe light so that $s_1=-9/\sqrt{15}$, $s_2=+5/4$, and $s_3=-\sqrt{15}/2$ (from Table I). The photolysis laser propagates along the laboratory Y-axis with the laser polarization in the X-Z plane, described by $E=45°$ [see Fig. 6(b)]. The probe laser is circularly polarized (the polarization direction is parallel to the propagation direction) so that $P=90°$ and $\Phi_{PE}=0°$. For slice imaging, $\Omega=90°$. Therefore, using Eqs. (17) and (18) we obtain

$$\cos\varepsilon = \frac{1}{\sqrt{2}}\cos\Theta, \quad \text{(B3a)}$$

$$\cos p = \cos\Theta, \quad \text{(B3b)}$$

$$\cos\varphi_{PE} = \frac{1}{\sqrt{2}}\sin^2\Theta/(\sin\varepsilon\sin p), \quad \text{(B3c)}$$

$$\sin\varphi_{PE} = \frac{1}{\sqrt{2}}\sin\Theta/(\sin\varepsilon\sin p). \quad \text{(B3d)}$$

Equation (B3) is inserted into Eq. (14), which yields the laboratory angular distribution, as a function of the angle Θ (the polar angle of the image). Notice that $\cos\varphi_{PE}$ and $\sin\varphi_{PE}$ are both inversely proportional to $(\sin\varepsilon\sin p)$, and that these factors always cancel when inserted in Eq. (14) so they never need to be evaluated. After factoring the resulting terms, the laboratory distribution can be expressed as

$$I(\Theta) = \left[1 - \frac{1}{4}\beta + \frac{1}{40}s_2(4A_0^2(\text{aniso}) + 4\,\text{Re}[A_1^2] - \text{Re}[A_2^2])\right] + \left[\frac{1}{2}\beta + s_2A_0^2(\text{iso}) - \frac{1}{56}s_2(6A_0^2(\text{aniso}) - 4\,\text{Re}[A_1^2] + \text{Re}[A_2^2])\right] P_2(\cos\Theta) + \left[\frac{1}{70}s_2(18A_0^2(\text{aniso}) - 12\,\text{Re}[A_2^2] + 3\,\text{Re}[A_2^2])\right] P_4(\cos\Theta) \pm \left[\frac{\sqrt{3}}{4}s_1\,\text{Im}[A_1^1] + \frac{1}{8\sqrt{2}}s_3\,\text{Im}[A_1^3](5\cos\Theta - 1)\right]\sin\Theta\cos\Theta, \quad \text{(B4)}$$

where the $\pm$ in the last term corresponds to the use of $\sigma_\pm$ circularly polarized probe light.

Equation (B4) can be written in the form

$$I(\Theta) = I_0[1 + \beta_2P_2(\cos\Theta) + \beta_4P_4(\cos\Theta) + \gamma_1\sin\Theta\cos\Theta + \gamma_3(5\cos^2\Theta - 1)\sin\Theta\cos\Theta] \quad \text{(B5)}$$

so that the four laboratory observables are γ_1, β_2, γ_3, and β_4, which can be expressed in terms of the seven parameters in Eq. (B4). For the exact determination of β and the six A_q^k parameters, data must be taken on a second detection transition (which will change the values of the s_k) or using at least two distinct laboratory geometries. The inversion of multiple parameters from several experimental geometries is discussed elsewhere.[35,57,59,84]

[1] J. P. Simons, J. Phys. Chem. **91**, 5378 (1987).
[2] P. L. Houston, J. Phys. Chem. **91**, 5388 (1987).
[3] R. N. Dixon, J. Chem. Phys. **85**, 1866 (1986).
[4] G. E. Hall and P. L. Houston, Annu. Rev. Phys. Chem. **40**, 375 (1989).
[5] R. N. Zare and D. R. Herschbach, Proc. IEEE **51**, 173 (1963).
[6] R. N. Zare, Ph.D. thesis, Harvard University, 1964.
[7] R. Bersohn and S. H. Lin, Adv. Chem. Phys. **16**, 67 (1969).
[8] T. P. Rakitzis, A. J. van den Brom, and M. H. M. Janssen, Chem. Phys. Lett. **372**, 187 (2003).
[9] C. A. Taatjes, M. H. M. Janssen, and S. Stolte, Chem. Phys. Lett. **203**, 363 (1993).
[10] A. G. Suits and O. S. Vasyutinskii, Chem. Rev. (Washington, D.C.) **108**, 3706 (2008).
[11] L. D. A. Siebbeles, M. Glass-Maujean, O. S. Vasyutinskii, J. A. Beswick, and O. Roncero, J. Chem. Phys. **100**, 3610 (1994).
[12] T. P. Rakitzis and R. N. Zare, J. Chem. Phys. **110**, 3341 (1999).
[13] R. N. Zare, *Angular Momentum: Understanding Spatial Aspects in Physics and Chemistry* (Wiley, New York, 1988).
[14] A. J. Orr-Ewing and R. N. Zare, Annu. Rev. Phys. Chem. **45**, 315 (1994).
[15] A. S. Bracker, E. R. Wouters, A. G. Suits, Y. T. Lee, and O. S. Vasyutinskii, Phys. Rev. Lett. **80**, 1626 (1998).
[16] Z. H. Kim, A. J. Alexander, S. A. Kandel, T. P. Rakitzis, and R. N. Zare, Faraday Discuss. **113**, 27 (1999).
[17] A. J. Alexander, Z. H. Kim, S. A. Kandel, R. N. Zare, T. P. Rakitzis, Y. Asano, and S. Yabushita, J. Chem. Phys. **113**, 9022 (2000).
[18] E. R. Wouters, M. Beckert, L. J. Russell, K. N. Rosser, A. J. Orr-Ewing, M. N. R. Ashfold, and O. S. Vasyutinskii, J. Chem. Phys. **117**, 2087 (2002).
[19] M. J. Bass, M. Brouard, A. P. Clark, C. Vallance, and B. Martinez-Haya, Phys. Chem. Chem. Phys. **5**, 856 (2003).
[20] T. P. Rakitzis and T. N. Kitsopoulos, J. Chem. Phys. **116**, 9228 (2002).
[21] T. P. Rakitzis, S. A. Kandel, and R. N. Zare, J. Chem. Phys. **108**, 8291 (1998).
[22] T. P. Rakitzis, S. A. Kandel, A. J. Alexander, Z. H. Kim, and R. N. Zare, Science **281**, 1346 (1998).
[23] T. P. Rakitzis, S. A. Kandel, A. J. Alexander, Z. H. Kim, and R. N. Zare, J. Chem. Phys. **110**, 3351 (1999).

[24] T. P. Rakitzis, P. C. Samartzis, R. L. Toomes, L. Tsigaridas, M. Coriou, D. Chestakov, A. Eppink, D. H. Parker, and T. N. Kitsopoulos, Chem. Phys. Lett. **364**, 115 (2002).
[25] T. P. Rakitzis, P. C. Samartzis, R. L. Toomes, T. N. Kitsopoulos, A. Brown, G. G. Balint-Kurti, O. S. Vasyutinskii, and J. A. Beswick, Science **300**, 1936 (2003).
[26] T. P. Rakitzis, P. C. Samartzis, R. L. Toomes, and T. N. Kitsopoulos, J. Chem. Phys. **121**, 7222 (2004).
[27] A. G. Smolin, O. S. Vasyutinskii, O. P. J. Vieuxmaire, M. N. R. Ashfold, G. G. Balint-Kurti, and A. J. Orr-Ewing, J. Chem. Phys. **124**, 094305 (2006).
[28] A. G. Smolin, O. S. Vasyutinskii, and A. J. Orr-Ewing, Mol. Phys. **105**, 885 (2007).
[29] A. J. Alexander, Z. H. Kim, and R. N. Zare, J. Chem. Phys. **118**, 10566 (2003).
[30] M. Brouard, R. Cireasa, A. P. Clark, F. Quadrini, and C. Vallance, Phys. Chem. Chem. Phys. **8**, 5549 (2006).
[31] K. O. Korovin, B. V. Picheyev, O. S. Vasyutinskii, H. Valipour, and D. Zimmermann, J. Chem. Phys. **112**, 2059 (2000).
[32] K. O. Korovin, A. A. Veselov, O. S. Vasyutinskii, and D. Zimmermann, Opt. Spectrosc. **93**, 530 (2002).
[33] K. O. Korovin, A. A. Veselov, E. M. Mikheev, O. S. Vasyutinskii, and D. Zimmermann, Opt. Spectrosc. **99**, 880 (2005).
[34] A. J. Alexander and T. P. Rakitzis, Mol. Phys. **103**, 1665 (2005).
[35] A. S. Bracker, E. R. Wouters, A. G. Suits, and O. S. Vasyutinskii, J. Chem. Phys. **110**, 6749 (1999).
[36] D. Sofikitis, L. Rubio-Lago, A. J. Alexander, and T. P. Rakitzis, Europhys. Lett. **81**, 68002 (2008).
[37] D. Sofikitis, L. Rubio-Lago, L. Bougas, A. J. Alexander, and T. P. Rakitzis, J. Chem. Phys. **129**, 144302 (2008).
[38] A. Brown, G. G. Balint-Kurti, and O. S. Vasyutinskii, J. Phys. Chem. A **108**, 7790 (2004).
[39] A. G. Smolin, O. S. Vasyutinskii, G. G. Balint-Kurti, and A. Brown, J. Phys. Chem. A **110**, 5371 (2006).
[40] A. T. J. B. Eppink, D. H. Parker, M. H. M. Janssen, B. Buijsse, and W. J. van der Zande, J. Chem. Phys. **108**, 1305 (1998).
[41] H. Sato, Chem. Rev. (Washington, D.C.) **101**, 2687 (2001).
[42] R. Vasudev, R. N. Zare, and R. N. Dixon, J. Chem. Phys. **80**, 4863 (1984).
[43] J. A. Beswick, M. Glass-Maujean, and O. Roncero, J. Chem. Phys. **96**, 7514 (1992).
[44] J. F. Black, E. Hasselbrink, J. R. Waldeck, and R. N. Zare, Mol. Phys. **71**, 1143 (1990).
[45] M. L. Costen and G. E. Hall, Phys. Chem. Chem. Phys. **9**, 272 (2007).
[46] M. L. Costen, S. W. North, and G. E. Hall, J. Chem. Phys. **111**, 6735 (1999).
[47] E. Hasselbrink, J. R. Waldeck, and R. N. Zare, Chem. Phys. **126**, 191 (1988).
[48] S. W. North and G. E. Hall, Chem. Phys. Lett. **276**, 103 (1997).
[49] M. Ahmed, D. S. Peterka, A. S. Bracker, O. S. Vasyutinskii, and A. G. Suits, J. Chem. Phys. **110**, 4115 (1999).
[50] M. Brouard, P. O'Keeffe, D. M. Joseph, and D. Minayev, Phys. Rev. Lett. **86**, 2249 (2001).
[51] M. Brouard, R. Cireasa, A. P. Clark, T. J. Preston, and C. Vallance, J. Chem. Phys. **124**, 064309 (2006).
[52] A. M. Coroiu, D. H. Parker, G. C. Groenenboom, J. Barr, I. T. Novalbos, and B. J. Whitaker, Eur. Phys. J. D **38**, 151 (2006).
[53] I. Wilkinson, M. P. de Miranda, and B. J. Whitaker, J. Chem. Phys. **131**, 054308 (2009).
[54] Y. X. Mo, H. Katayanagi, M. C. Heaven, and T. Suzuki, Phys. Rev. Lett. **77**, 830 (1996).
[55] T. Suzuki, H. Katayanagi, S. Nanbu, and M. Aoyagi, J. Chem. Phys. **109**, 5778 (1998).
[56] Z. H. Kim, A. J. Alexander, and R. N. Zare, J. Phys. Chem. A **103**, 10144 (1999).
[57] T. P. Rakitzis, P. C. Samartzis, and T. N. Kitsopoulos, Phys. Rev. Lett. **87**, 123001 (2001).
[58] S. K. Lee, R. Silva, S. Thamanna, O. S. Vasyutinskii, and A. G. Suits, J. Chem. Phys. **125**, 144318 (2006).
[59] M. Brouard, A. V. Green, F. Quadrini, and C. Vallance, J. Chem. Phys. **127**, 084304 (2007).
[60] M. Brouard, F. Quadrini, and C. Vallance, J. Chem. Phys. **127**, 084305 (2007).
[61] M. Brouard, A. P. Clark, C. Vallance, and O. S. Vasyutinskii, J. Chem. Phys. **119**, 771 (2003).
[62] D. W. Neyer, A. J. R. Heck, D. W. Chandler, J. M. Teule, and M. H. M. Janssen, J. Phys. Chem. A **103**, 10388 (1999).
[63] A. G. Smolin, O. S. Vasyutinskii, E. R. Wouters, and A. G. Suits, J. Chem. Phys. **121**, 6759 (2004).
[64] T. Suzuki, H. Katayanagi, Y. X. Mo, and K. Tonokura, Chem. Phys. Lett. **256**, 90 (1996).
[65] J. M. Teule, G. C. Groenenboom, D. W. Neyer, D. W. Chandler, and M. H. M. Janssen, Chem. Phys. Lett. **320**, 177 (2000).
[66] M. Brouard, R. Cireasa, A. P. Clark, G. C. Groenenboom, G. Hancock, S. J. Horrocks, F. Quadrini, G. A. D. Ritchie, and C. Vallance, J. Chem. Phys. **125**, 133308 (2006).
[67] W. Denzer, S. J. Horrocks, P. J. Pearson, and G. A. D. Ritchie, Phys. Chem. Chem. Phys. **8**, 1954 (2006).
[68] G. Hancock, S. J. Horrocks, P. J. Pearson, G. A. D. Ritchie, and D. F. Tibbetts, J. Chem. Phys. **122**, 244321 (2005).
[69] G. Hancock, P. J. Pearson, G. A. D. Ritchie, and D. F. Tibbetts, Phys. Chem. Chem. Phys. **5**, 5386 (2003).
[70] G. Hancocks, P. J. Pearson, G. A. D. Ritchie, and D. F. Tibbetts, Chem. Phys. Lett. **393**, 425 (2004).
[71] S. J. Horrocks, P. J. Pearson, and G. A. D. Ritchie, J. Chem. Phys. **125**, 133313 (2006).
[72] S. J. Horrocks, G. A. D. Ritchie, and T. R. Sharples, J. Chem. Phys. **127**, 114308 (2007).
[73] S. K. Lee, D. Townsend, O. S. Vasyutinskii, and A. G. Suits, Phys. Chem. Chem. Phys. **7**, 1650 (2005).
[74] A. J. Alexander, Phys. Rev. A **66**, 060702 (2002).
[75] A. J. Alexander, J. Chem. Phys. **118**, 6234 (2003).
[76] M. Brouard, R. Cireasa, A. P. Clark, T. J. Preston, C. Vallance, G. C. Groenenboorn, and O. S. Vasyutinskii, J. Phys. Chem. A **108**, 7965 (2004).
[77] V. V. Kuznetsov and O. S. Vasyutinskii, J. Chem. Phys. **123**, 034307 (2005).
[78] V. V. Kuznetsov and O. S. Vasyutinskii, J. Chem. Phys. **127**, 044308 (2007).
[79] P. S. Shternin and O. S. Vasyutinskii, J. Chem. Phys. **128**, 194314 (2008).
[80] V. V. Kuznetsov, P. S. Shternin, and O. S. Vasyutinskii, J. Chem. Phys. **130**, 134312 (2009).
[81] V. V. Kuznetsov, P. S. Shternin, and O. S. Vasyutinskii, Phys. Scr. **80**, 048107 (2009).
[82] Y. Mo and T. Suzuki, J. Chem. Phys. **112**, 3463 (2000).
[83] T. P. Rakitzis, S. A. Kandel, and R. N. Zare, J. Chem. Phys. **107**, 9382 (1997).
[84] T. Peter Rakitzis, Chem. Phys. Lett. **342**, 121 (2001).
[85] M. P. Docker, Chem. Phys. **185**, 125 (1988).
[86] C. H. Greene and R. N. Zare, J. Chem. Phys. **78**, 6741 (1983).
[87] A. C. Kummel, G. O. Sitz, and R. N. Zare, J. Chem. Phys. **85**, 6874 (1986); **88**, 6707 (1988).
[88] Y. Mo and T. Suzuki, J. Chem. Phys. **109**, 4691 (1998).
[89] T. P. Rakitzis and M. H. M. Janssen, Mol. Phys. **108**, 937 (2010).
[90] K. H. Gericke, S. Klee, F. J. Comes, and R. N. Dixon, J. Chem. Phys. **85**, 4463 (1986).
[91] R. Uberna, R. D. Hinchliffe, and J. I. Cline, J. Chem. Phys. **103**, 7934 (1995).
[92] K. M. Chen and C. C. Pei, J. Chem. Phys. **110**, 7256 (1999).
[93] M. P. Docker, Chem. Phys. **405**, 135 (1989).